ChemBioChem

Combining Chemistry and Biology

Chemistry Europe

European Chemical Societies Publishing

Accepted Article

Title: Environmentally Friendly Degradation and Detoxification of Rifampicin by a Bacterial Laccase and Hydrogen Peroxide

Authors: Paulo Durao, Peter Kis, Ivo M. Chelo, M. Rita Ventura, and Lígia O. Martins

To be cited as: *ChemBioChem* **2023**, e202300627

Link to VoR: https://doi.org/10.1002/cbic.202300627

WILEY VCH

10.1002/cbic.202300627

Environmentally Friendly Degradation and Detoxification of Rifampicin by a Bacterial Laccase and Hydrogen Peroxide

Paulo Durão[1‡], Peter Kis[1], Ivo M. Chelo[2,3], M. Rita Ventura[1] and Lígia O. Martins[1]

[1] *Instituto de Tecnologia Química e Biológica António Xavier, Universidade Nova de Lisboa, Av da República, 2780-157 Oeiras Portugal*

[2] *cE3c – Centre for Ecology, Evolution and Environmental Changes & CHANGE – Global Change and Sustainability Institute, Lisboa, Portugal*

[3] *Departamento de Biologia Animal, Faculdade de Ciências, Universidade de Lisboa, Lisboa, Portugal*

Running title: Chemo-enzymatic degradation of rifampicin

Correspondence[‡]: Paulo Durão, pdurao@itqb.unl.pt

ABSTRACT

Antibiotics are micropollutants accumulating in our rivers and wastewaters, potentially leading to bacterial antibiotic resistance, a worldwide problem to which there is no current solution. Here, we have developed an environmentally friendly two-step process to transform the antibiotic rifampicin (RIF) into non-antimicrobial compounds. The process involves an enzymatic oxidation step by the bacterial CotA-laccase and a hydrogen peroxide bleaching step. NMR identified rifampicin quinone as the main product of the enzymatic oxidation. Growth of *Escherichia coli* strains in the presence of final degradation products (FP) and minimum inhibitory concentration (MIC) measurements confirmed that FP are non-anti-microbial compounds, and bioassays suggest that FP is not toxic to eukaryotic organisms. Moreover, competitive fitness assays between susceptible and RIF-resistant bacteria show that susceptible bacteria is strongly favoured in the presence of FP. Our results show that we have developed a robust and environmentally friendly process to effectively remediate rifampicin from antibiotic contaminated environments.

INTRODUCTION

Antibiotics are key in the clinical treatment of infections and growth promotion of animal livestock. However, their continuous discharge into the environment, together with the low rates of degradation of some of them, is making antibiotics accumulate and become a new micro-pollutant, which are currently poorly legislated [1,2]. Moreover, the accumulation of antibiotics has the potential to generate reservoirs of antibiotic-resistant bacterial strains since the presence of these drugs in the environment strongly promotes the evolution of these strains [3,4], even at very low concentrations [5,6]. Antibiotic resistance is a growing, widespread problem, with antibiotic-resistant infections causing in 2019 almost 1.3 million deaths worldwide and a huge economic burden [7]. Nevertheless, there are fewer and fewer antibiotics with novel modes of action available in the market and it is currently non-attractive for companies to spend resources in research to develop new antibiotics [8]. Moreover, the use of novel antibiotics will likely result in an increased level of antibiotics in the environment and maintain the selection pressure favouring resistance.

Current antibiotic bioremediation relies on technologies such as photocatalysis, membrane filtration, activated carbon adsorption, chlorination and advanced oxidation processes [9]. Most biological strategies involve the use of activated sludge whereas an unspecific community of microbes metabolizes the antibiotics. Although this solution is cheap, its performance is highly variable, poorly understood and the determinants of the reaction are often determined empirically in a labour-intensive process [10,11]. By comparison, enzymatic biodegradation is still a mildly explored alternative to detoxify some antibiotics such as tetracyclines, β-lactams, rifampicin, and others [12–14] but may allow for a greater level of reproducibility, increasing its applicability.

Rifampicin (also known as (3-(4-methylpiperazinyliminomethyl) rifamycin SV), RIF throughout the manuscript) is a semisynthetic aromatic antibiotic important to treat

tuberculosis, since it is one of the very few antibiotics capable of killing slow-growing microorganisms as *Mycobacterium tuberculosis* [15]. RIF binds and inhibits bacterial RNA polymerase [16] and its intensive use has led to the wide spread of resistance which is mainly associated to chromosomal mutations in the RNA polymerase gene(s) [17]. RIF has a heterocyclic structure containing a naphthyl core, giving its characteristic red/orange colour and it is mostly recalcitrant to degradation. RIF display pigment properties and often non-metabolized RIF is excreted, making patients under treatment display secondary effects as red or orange urine, saliva and tears. Due to its properties, RIF accumulating in the environment has the potential to negatively impact the microbial soil ecosystems while selecting for resistant bacteria.

Laccases are multicopper proteins interesting for the biodegradation of antibiotics because they are known to catalyse the mono-electronic oxidation of a wide range of phenolic and aromatic substrates, with their only by-product being water [18,19]. The catalytic mechanism of laccases involves (1) reduction of the T1 Cu site by the oxidized substrate, (2) electron transfer from the T1 Cu site to the trinuclear centre and (3) O_2 reduction by the trinuclear cluster [18,19]. Whereas fungal laccases have been shown to degrade some antibiotics [20] this was not demonstrated to bacterial counterparts that furthermore has advantages such as an improved thermostability and activity in a wider range of pHs [21,22]. CotA-laccase has a known three-dimensional structure and has been used as a model protein for structure-function, protein engineering and application studies [18,19,23].

In here, we have firstly characterized the ability of purified CotA-laccase to transform the antibiotic rifampicin into a single product that was identified by NMR to be rifampicin quinone (RFQ). RFQ still held antimicrobial properties and strong purple colouration but adding hydrogen peroxide subsequently bleached it into colourless final degradation non-antimicrobial products (FP), as assessed by measuring the minimum inhibitory concentrations

(MICs) for an *Escherichia coli* strain susceptible to rifampicin. Moreover, growth curves and competitive fitness assays supplemented with FP show that rifampicin resistant strains do not benefit from the presence of FP. Finally, toxicity assays with the model organism *C. elegans* suggest that FP are also not toxic to eukaryotic organisms.

MATERIAL AND METHODS

Chemicals, strains and growth conditions

Rifampicin was obtained from Sigma Aldrich (CAS# 13292-46-1) with a 95% purity, according to the manufacturer. A 10 mg/ml rifampicin stock solution was prepared in 96% methanol and thereafter further dilutions were all made in 100 mM phosphate buffer. Hydrogen peroxide was obtained from Sigma. *E. coli* Tuner(DE3)pLacI (Novagen) strain AH3517, carrying the *cotA* gene under the control of an inducible IPTG plasmid, was used to overexpress CotA [22]. AH3517 was first grown aerobically in Luria–Bertani (LB) medium supplemented with ampicillin (100 μg mL^{-1}) with 120 rpm shaking (Innova1 44, New Brunswick Scientific). The cells were grown at 30ºC until an optical density at 600nm (OD_{600nm}) of 0.6 was reached, after which 0.1 mM isopropyl-β-D-thiogalactopyranoside (IPTG) and 0.25 mM $CuCl_2$ were added to the culture medium and the temperature was reduced to 25ºC. Incubation continued for a further 4 h and then a change to microaerobic conditions was achieved by switching off the shaking function, as described previously [21]. Cells were harvested after a further 20 h of growth by centrifugation. Cell disruption and a two-step protein purification chromatographic procedure were conducted as previously described [22]. Protein concentration was measured either by using the absorption band at 280 nm (ε_{280nm} =84,739 $M^{-1}cm^{-1}$) or by the Bradford method. The amount of copper bound to CotA was determined through the trichloroacetic acid/bicinchoninic acid method of Brenner and Harris [24], yielding a ≈ 4:1 ratio of copper per protein.

Enzyme assays

The laccase-catalysed oxidation reactions of rifampicin were photometrically monitored with either a Shimadzu UV-1603 spectrophotometer or a Biotek Epoch 2 microplate reader with a 96-well plate. The molar extinction coefficients of rifampicin (in the concentration range of 0.2 –0.02 µg/mL) were determined at the maximal wavelength of 470 nm at pHs ranging from 4 to 8 and, therefore, all oxidation reactions of rifampicin were followed at 470 nm (ε = 12676 M^{-1} cm^{-1}). The effect of pH on the enzyme activity was determined at 37ºC using Britton–Robinson (BR) buffer (100 mM phosphoric acid, 100 mM boric acid and 100 mM acetic acid mixture with 0.5 M NaOH to the desired pH) ranging from pH 3-10. The apparent kinetic parameters (k_{cat} and K_M) towards rifampicin oxidation were determined at 470 nm (ε_{470nm} = 12676 M^{-1} cm^{-1}) in a discontinuous assay due to the high extinction coefficient at this wavelength, at 37ºC in phosphate buffer pH 6. The kinetic parameters were determined by directly fitting a Michaelis-Menten equation using the function MM.2 in the "drc" package (R software). All enzymatic assays were performed at least in triplicate.

Hydrogen peroxide bleaching

The concentration of the hydrogen peroxide stock solution was calculated from its absorption at 240 nm using a ε = 43.6 $M^{-1}.cm^{-1}$ [25]. Bleaching reactions were set up by diluting a 30% stock solution (Sigma) and 0.2 mg/ml of RFQ bleaching was followed spectrophotometrically at $\lambda \approx 535$ nm (ε_{535nm} = 2995 $M^{-1}.cm^{-1}$) at 37ºC for 1h. Epsilon at λ = 535 nm was determined beforehand by scanning the spectra of several concentrations of RFQ (Figure S1).

Characterization of the reaction products by TLC and NMR

All reactions were monitored on TLC plates (Silicagel 60, F_{254}). The spots of compounds were detected with UV lamp (λ_{max} = 254 nm or 366 nm). To obtain pure CotA oxidation product for NMR characterization, a standard preparative scale reaction was set up. RIF (82.3 mg, 0.1 mmol) was dissolved in methanol (8.2 mL) and then diluted with phosphate buffer (100 mM, pH 6, 73.8 mL) and CotA (0.1 mg/mL) was added. The reaction mixture was incubated at 37 ºC with 600 rpm agitation for 30 minutes until TLC samples (dichloromethane/methanol = 12:1 (v/v)) showed complete conversion of RIF to RFQ. Afterwards, the reaction mixture was diluted with water (50 mL) and extracted with dichloromethane (4x 100 mL). Afterwards, the reaction mixture was diluted with water and extracted with dichloromethane (4x). The organic fraction was dried over anhydrous magnesium sulphate and evaporated to dryness. The resulting purple amorphous crude product was purified on silica using dichloromethane/methanol = 12:1 (v/v) to obtain pure RFQ as a burgundy coloured amorphous solid (70 mg, 85%).

Column chromatography was performed on Silica gel 60A (40–63 µm). Spectra were acquired at 25°C on a Bruker Avance III 800 spectrometer (Bruker, Rheinstetten, Germany) working at a proton operating frequency of 800.33 MHz, equipped with a 5 mm, three channel, inverse detection cryoprobe TCI-z H&F/C/N with pulse-field gradients. Shifts are referenced to internal solvents or Me4Si as internal standard, respectively. ^{13}C NMR spectra were recorded at 201.26 MHz and shifts are referenced to internal solvents. Chemical shifts are expressed in parts per million (d scale) downfield from tetramethylsilane and are referenced to the residual proton in the NMR solvent (CDCl3: δ 7.26 ppm, δ 77.23 ppm). For correct complete assignment of signals a two-dimensional homonuclear correlation technique (H-H COSY), heteronuclear correlation techniques (H-C HSQC, HMBC and H2BC) were performed. High resolution mass spectrometry data was obtained by the Mass Spectrometry Unit (UniMS), ITQB/iBET, Oeiras, Portugal.

158

159 **Measurement of the minimum inhibitory concentrations (MICs)**

160 Strains used to determine the MICs are derivatives of an *E. coli* K12 MG1655, which
161 constitutively express yellow (YFP) fluorescent proteins inserted in the galK locus and had the
162 entire lac operon deleted (Δ*lacIZYA galK::cat::PLlacO-1-YFP*). Resistant mutants also
163 harbour chromosomal resistance mutations to rifampicin ($RpoB^{H526Y}$, $RpoB^{S512F}$, $RpoB^{S531F}$
164 and $RpoB^{I572F}$ alleles). To determine the MICs of rifampicin and the degradation compounds,
165 the compounds were diluted in Mueller-Hinton media ranging from 1000 µg/mL to 3 µg/mL
166 [1000, 500, 250, 100, 50, 20, 10, 5, 3, 0 µg/mL]. Since H_2O_2 is a powerful disinfectant, FP was
167 beforehand supplemented with catalase (30 µg/mL) for 24h to remove H_2O_2 in excess. Pure
168 cultures of the strains were grown in Mueller-Hinton broth and the culture was standardized by
169 OD_{600nm} to have a concentration of $\approx 10^6$ cells/ml in the final well. The 96-well plates with the
170 inoculated wells were incubated at 37 ºC for around 18 h. After incubation, the series of
171 dilutions were observed for microbial growth (turbidity). The last tube in the dilution series
172 that does not demonstrate growth corresponds to the MIC of tested compound.

173

174 **Growth curves**

175 *E. coli* growth was assessed in 96-well plates using a 200 µl growth assay in a Bioscreen C
176 Microbiology Reader (Growth Curves Ltd, Finland). Growths were performed in LB media
177 supplemented with catalase (30 µg/mL) to remove traces of H_2O_2 from FP (previously treated
178 with catalase for 24 h) and started with ≈106 cells/mL. The OD600nm of cultures in the
179 Bioscreen was measured every 30 min for 24 h with continuous shaking (aeration) at 37 ºC.
180 Maximum growth rates were calculated using R package "growthrates" using the
181 "all_easylinear" function which determines maximum growth rates from the log-linear part of
182 the growth curve. A minimum of four independent assays were done for each resistant clone.

183

184 **Competitive fitness in the presence of degradation products**

185 The relative fitness between *E. coli* susceptible to antibiotics (*E. coli* K12 MG1655) and the
186 rifampicin resistant strains was measured by mixing 50% of YFP or CFP resistant strain with
187 50% of the CFP or YFP reference strain and each mixed population was allowed to compete
188 for 24 h. The initial and final frequency of the strains was obtained by counting their cell
189 numbers in LB plates without antibiotic (total colonies) and by counting the resistant cell
190 numbers by plating in LB supplemented with rifampicin (100 μg/mL). Relative fitness,
191 representing the selection coefficient (S), of each mutant strain was estimated as the per
192 generation difference in Malthusian parameters: $S = \ln(R_f/R_i)/t$, where t is the number of
193 generations after 24h growth for the susceptible strain and R_f and R_i are the final and initial
194 ratios between resistant and reference strain, respectively. Generation time was estimated from
195 the doubling time of the reference strain (approximately eight generations/24 h). Values
196 represent the average of at least three independent replicates for each competition.

197

198 **Toxicity assays with eukaryotic organism *C. elegans***

199 Biological toxicity of the final degradation compounds was tested with *C. elegans*, following
200 Bischof's and colleagues L1 growth assay [26]. In this assay, the development of first-larval
201 staged *C. elegans* individuals (L1s) into pre-adult larvae (fourth-staged larvae, L4s) is analysed
202 under different test conditions. Groups of 60 to 80 L1s were initially placed in single wells of
203 24 well-plates and, 60 hours later, the number of individuals surviving past L1 stage, and their
204 body sizes (body area) were recorded as measures of successful development. These were
205 obtained by direct (visual) inspection and counting, for the number of surviving individuals, or
206 by acquisition of worm images with a stereoscope and digital camera, and analysis with
207 ImageJ. The assay was done at 20º C, in liquid media (M9 buffer), *E. coli* OP50 and tetracycline

at 25 µg/ml defining the positive control conditions. The absence of food was used as the negative control. Test conditions included H_2O_2 [1 mM], the antibiotic rifampicin at 100 µg/ml, and FP also at 100 µg/ml. The effect of catalase was also tested at a final concentration of 25 µg/ml. Each estimate was done based on three replicates and statistical analysis was conducted in R. Significance testing against the positive control and confidence intervals were obtained in a model where each treatment was used as a predictor. For the analysis of body size, log transformation was used to normalize the error at different predictor scales. Tukey's HSD correction was used with the *emmeans* and *contrast* functions, in R for multiple test correction.

RESULTS AND DISCUSSION

CotA laccase oxidizes rifampicin

CotA-laccase was overexpressed by an *E. coli* Tuner strain and then purified as previously described [22]. Oxidation of rifampicin was observed by the change of colour of the reaction mixture from orange to purple (Figure 1A). The UV-spectra of the final reaction shows a decrease at ≈ 460-470 nm and an increase of absorbance at 395 and 535 nm, corresponding to the decrease of substrate rifampicin and an increase of oxidized purple product, respectively. Since the naphthyl core is usually associated with the colour of this compound with peaks in UV-visible region, our data suggests that the product was oxidized in the vicinities of the aromatic ring of the naphthyl core, thus indicating that the final product may be rifampicin quinone (RFQ). Indeed, in the oxidation of rifampicin by horseradish peroxidase, RFQ was proposed as the final product [27] but confirmatory structural data was missing.

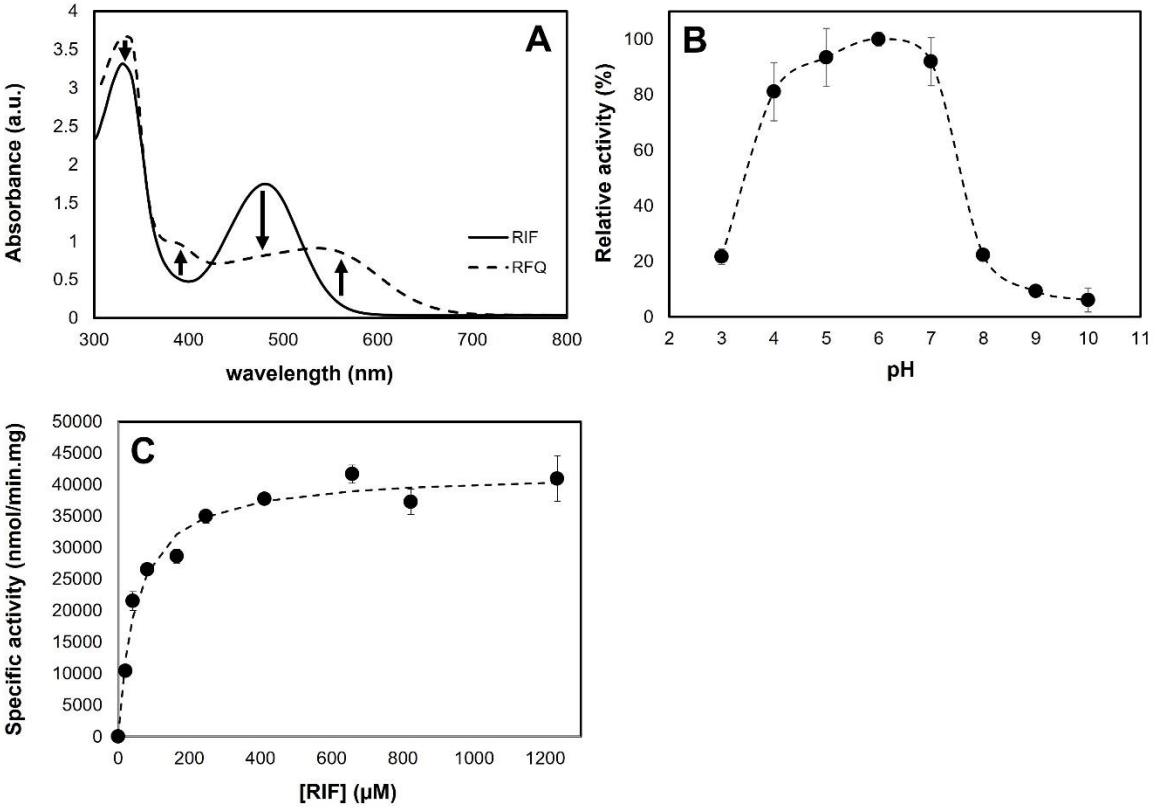

Figure 1 – CotA laccase oxidation of rifampicin. **A)** Absorbance spectra of 0.2 mg/mL of rifampicin (RIF; full line) and the product of the enzymatic oxidation of RIF by CotA-laccase at pH 6, 37ºC for 5 min (dashed line). The aromatic ring of RIF gives a bright orange colour at this concentration (peak at $\lambda \approx 460 - 470$ nm), while the product has a purple colour ($\lambda \approx 535$ nm), suggesting a change in the vicinity of the naphthyl core. **B)** pH profile of the CotA-laccase oxidation of RIF in 100 mM Britton-Robinson buffer. CotA displays a bell-shaped pH profile with an optimum at pH 6. **C)** CotA-laccase activity [pH 6, 37ºC] was determined for several concentrations of RIF and the efficiency (k_{cat}/K_M) was determined to be $(9.02 \pm 1.88) * 10^5$ $M^{-1}.s^{-1}$ by a Michaelis-Menten fit corresponding to a $k_{cat}^{app} = 45 \pm 1$ s^{-1} and a $K_M^{app} = 50 \pm 5$ µM.

To follow spectrophotometrically the enzymatic reaction by substrate consumption, we have determined the extinction coefficient of rifampicin at the maximal absorption band ≈ 470nm (ε_{470nm}) in the UV-visible spectrum (Figure S1). The same $\varepsilon_{470nm} \approx 12{,}676$ $M^{-1}cm^{-1}$ was obtained from pH 4 to pH 8 but linearity is restricted to a limited range of concentrations of RIF (between 16.5 µM and 165 µM corresponding to 0.02 and 0.2 µg/mL, respectively). The pH profile for the CotA-laccase oxidation of RIF (Figure 1B) is bell-shaped with an optimal at pH 6, displaying a plateau of maximal activity between pH 5 and 7; at pH 4 the enzyme still

holds 80% activity. Thus, CotA-laccase performs this reaction optimally at neutral to slightly acidic pHs which is interesting for future wastewater treatment plants (WWTP) applications since the current microbial bioremediation techniques are most effective at pH close to neutral. We have then determined the apparent k_{cat}/K_M of the enzyme reaction to be $9.02 * 10^5$ $M^{-1}.s^{-1}$ by a Michaelis-Menten fit (Figure 1C) corresponding to a k_{cat}^{app} of $\approx 45 \pm 1$ s^{-1} and a K_M^{app} of 50 ± 5 µM. CotA laccase presents a ≈ 9-fold faster turnover and a ≈ 2-fold higher affinity towards RIF when in comparison with HRP ($k_{cat}^{app} = 5.1 \pm 0.6$ s^{-1}, and $K_M^{app} = 101 \pm 23$ µM), indicating that CotA laccase has a ≈ 20-fold better efficiency towards rifampicin oxidation than HRP [27].

Hydrogen peroxide bleaches RFQ

Hydrogen peroxide (H_2O_2) is a known disinfectant often used in WWTPs [28]. It is also a known powerful bleaching agent commonly used in dentistry or the textile industry [29,30]. Importantly, hydrogen peroxide at low concentrations is considered safe to drink and is eco-friendly since it breaks down to water and oxygen. Thus, we have tested the ability of hydrogen peroxide to damage the chromogenic group of RFQ. The addition of 100 mM H_2O_2 to 0.2 mg/mL solution of RFQ quickly resulted in final products with loss of colouration (denominated FP from now on, Figure 2A) after 10 min reaction at 37ºC, pH 6. Contrary to RIF and RFQ, which display clear peaks in the UV-visible region (peaks at λ ≈ 470 and 535 nm to RIF and RFQ, respectively), FP displays no clear peak in the visible region between 400 and 750 nm suggesting a change or loss of the naphthyl core (Figure 2A).

Next, to be able to follow spectrophotometrically the RFQ consumption during the reaction, we have determined the extinction coefficient at the maximal band in the UV-visible region (λ = 535 nm) to be 2995 $M^{-1}.cm^{-1}$. We then studied the effect of pH and temperature in the bleaching process of RFQ [31] (Figure 2B-C). The optimal pH for RFQ degradation was ≈ pH

9 (Figure 2B). The reaction was similarly fast at higher pHs, but the UV-visible spectra of RFQ were distinct in this range of pHs and did not allow a proper spectrophotometric quantification at 535nm (data not shown). The increase of bleaching between pH 4 to 9 is almost linear (linear regression fit given by $y = 20.257x - 81.592$, $r^2 = 0.9412$; Figure 2B, inset), suggesting a 20% linear increase of activity for each increase of pH unit in this pH range. On the other hand, adding 100 mM H_2O_2 to a solution of 0.2 mg/mL of RIF in a pH range between 3 to 10 did not change the UV-visible spectra neither showed any decrease at 470 nm (37ºC, 10 min reactions). The optimal reaction temperature at pH 9 was around 55ºC (100 ± 12 % activity, Figure 2C). The linear increase of bleaching activity at basic pHs and higher temperatures suggests that H_2O_2 bleaching occurs through the generation of reactive oxygen species (ROS) during the decomposition hydrogen peroxide into water (equations 1-3, [32]).

$$H_2O_2 \rightarrow H^+ + HO_2^- \quad (1)$$

$$HO_2^- + H_2O_2 \rightarrow (HO^\bullet_2) + HO^\bullet + OH^- \quad (2)$$

$$HO^\bullet + H_2O_2 \rightarrow HO^\bullet_2 + H_2O \quad (3)$$

Bleaching reactions at increasing concentrations of RFQ in the presence of H_2O_2 reveal a linear increase of RFQ bleached at 37 ºC and pH 9 (Figure 2D). Thus, the rate of the reaction can be calculated for any concentration of reactant by the formula rate = $4*10^{-6}$ x [RFQ]x[H_2O_2], consistent with a second order reaction. The bleaching in these conditions is the rate-limiting step of the degradation pathway of RIF into non-antimicrobial compounds since it is significantly slower than the enzymatic RIF oxidation.

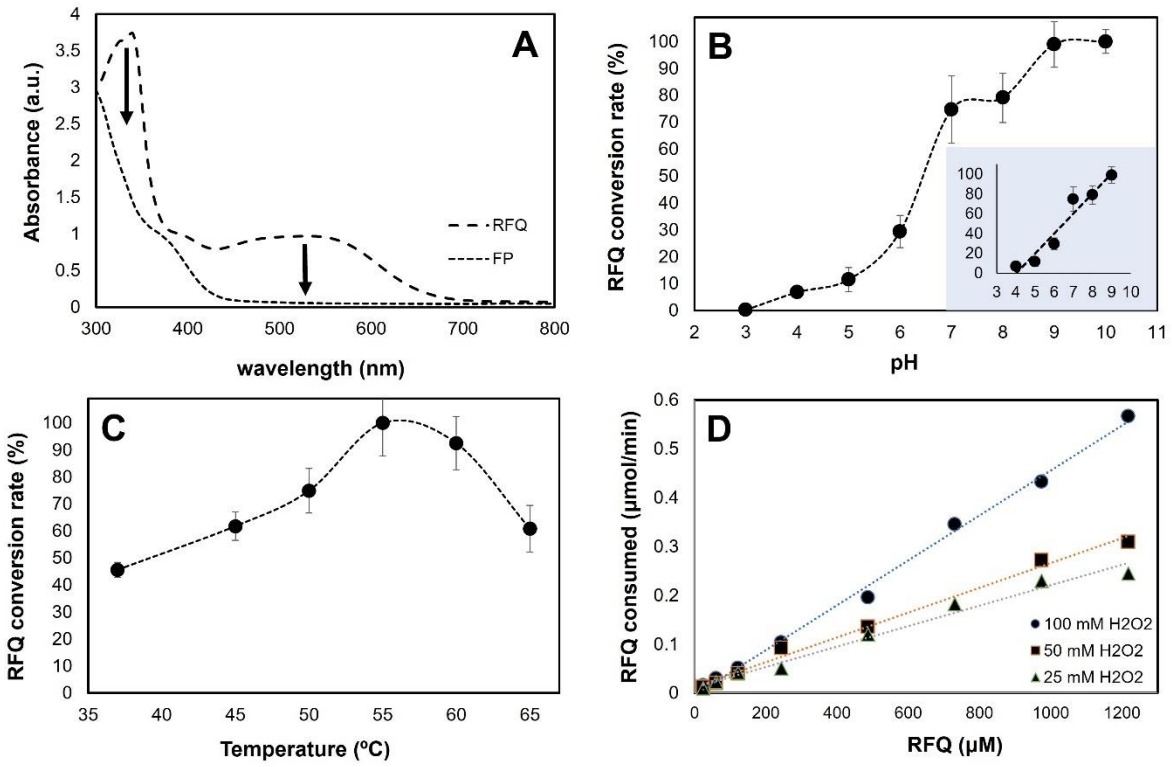

Figure 2 – Rifampicin quinone is bleached by hydrogen peroxide. **A)** Absorbance spectra of the 0.2 mg/mL of CotA-laccase oxidation products (RFQ; dashed line) and the final product after reacting with 100 mM of H_2O_2 at pH 9, 37ºC for 10 min (FP; dotted line, RFQ). FP is pale yellow with no clear peak in the UV-visible suggesting either further changes or even the loss of the aromatic ring. **B)** pH profile of the H_2O_2 conversion rate of RFQ in 100 mM Britton-Robinson buffer. The reaction displays an optimum pH of 9. There is a linear correlation between pH 4 to 9 and the bleaching activity of H_2O_2. **C)** Optimal temperature of the H_2O_2 mediated conversion rate of RFQ is around 55ºC. **D)** Linear co-dependence of the bleaching conversion rate on the amount of the RFQ and H_2O_2 substrates suggests a second order reaction. Bleaching rate of RFQ is directly dependent of the concentration of both reactants and the rate of the reaction can be calculated for any concentration of reactant by the formula rate = $4*10^{-6}$ x [RFQ]x[H_2O_2], whereas the slope stands for the µmol of RFQ bleached per mM of H_2O_2 per minute.

Characterization of the degradation products

NMR identification of the CotA laccase oxidation product

We have characterized the products of the CotA-laccase RIF oxidation by thin layer chromatography (TLC) and NMR. TLC of RIF shows a main orange band corresponding to the antibiotic itself but also a purplish impurity consistent with the 95% purity of the purchased compound (Figure S2). After enzymatic RIF oxidation there was no traces of RIF in the TLC

and only one single product band with the same retention time and purplish colour as the impurity present in RIF is present, suggesting that it is the same compound (Figure S2). For NMR characterization, pure RIF oxidation product was further purified (see Material Methods section). By combining a range of ^{1}H- and ^{13}C-NMR techniques (APT, COSY, HSQC, HMBC and H2BC) in $CDCl_3$ at 800 MHz and 201 MHz, respectively, we were able to identify CotA-laccase oxidized product as being RFQ (Figure 3, Table I and Supplemental Material). Accordingly, high-resolution mass spectrometry has yield an observed $[M+H]^+$ strongly in agreement with the calculated for RFQ (821.3973 versus 821.3971 for calculated and measured values, respectively; Figure S3). To our knowledge, this is the first time that the complete spectrum of RFQ is published in the literature [33,34].

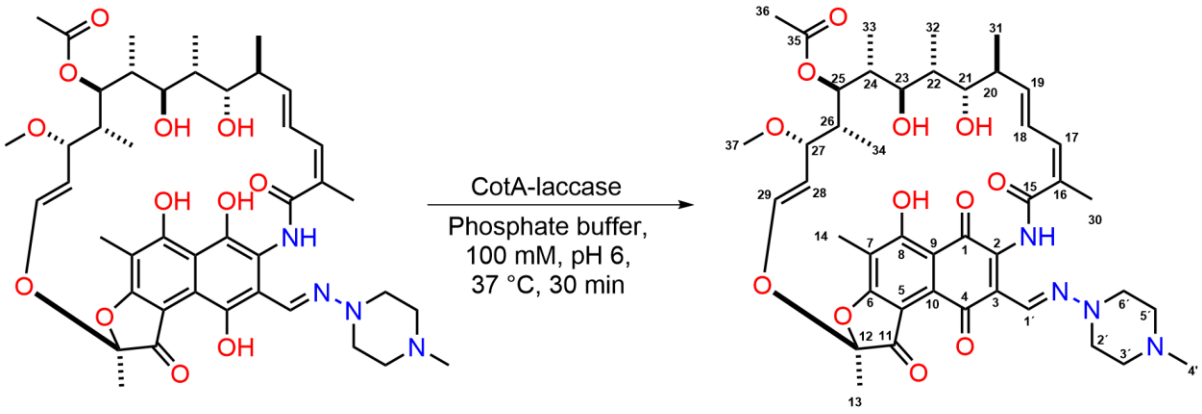

Figure 3 - Reagents and conditions for CotA-laccase catalysed oxidation of RIF to RFQ.

In the ^{1}H-NMR analysis of CotA-laccase oxidation product, the key protons H-17, H-18, H-19, H-28, and H-29 were assigned (for details please see Supplemental Information, Table I and Supplemental Figure S4). Notably, H-17 showed significant allyl coupling to methyl H-30 and proton H-29 exhibited allyl coupling with H-27 and simultaneous coupling to H-28. Incomplete resolution of multiplets complicated assignment of protons H-20 to H-27. The COSY spectrum revealed correlations between H-26 and methyl H-34. The ansa-ring's H-26 proton correlated with H-25, which correlated with H-24. Assigning H-32 and H-33 methyl groups proved challenging due to signal overlap. Chemical shifts for carbons C-17, C-18, C-

19, C-21, C-23, C-25, C-26, C-27, C-28, C-29, and C-31 were determined using the HSQC spectrum. H-33 methyl group was identified via the HMBC spectrum, and H-24 assignment relied on H2BC and HSQC spectra. Proton H-17 had a strong correlation with C-15. H-25 correlated with C-35 in the HMBC spectrum, aiding identification of methyl carbon C-37. HMBC correlations between H-29, H-28, and C-12, along with interactions with methyl H-13 and carbonyl carbon C-11, were observed. The assignment process extended to H-20, revealing C-20 in the HSQC spectrum. Correlations in HMBC facilitated identification of C-22, H-32, H-14, C-14, and signals in the N-methylpiperazine ring. Assigning quaternary carbon signals in the naphthoquinone part involved HMBC interactions with H-1', H-14, and H-30. H-1' correlations indicated C-2, C-3, C-1, and C-4. H-14 correlated with C-8, C-6, and C-7. Comparison with rifamycin derivatives' NMR spectra[35] aided C-9 and C-10 assignment. A signal at 130.28 ppm without H-1' correlation was identified as C-5.

For longer oxidation periods (≥ 3 h), it was occasionally visible on the TLCs a second band with an almost identical retardation factor of RFQ (R_f = 0.61 vs R_f^{RFQ} = 0.57, respectively) (Figure S5). Purification of such a reaction mixture on preparative TLC (dichloromethane/methanol = 15:1 (v/v), developed three times) afforded a new purple product which we called RFQ^{II}. Comparison of the ^{1}H-NMR spectra of RFQ and RFQ^{II} (Table I and Table SI, respectively) showed only small changes in the chemical shifts of most signals (0.2-0.3 ppm). More pronounced changes in the chemical shifts of the signals were observed only in the case of H-18 (0.48 ppm), H-24 (0.52 ppm) and H-26 (0.72 ppm) (Table I and Table SI). Overall, the NMR spectra indicates that the isolated compound is chemically identical to RFQ, except to a different conformation of the ansa-ring. This is the first report of RFQ to exist in two different conformations either in aqueous buffer or in $CDCl_3$ [33]. The relatively large change in the chemical shift of the H-18 proton is apparently a consequence of the anisotropic effect of the amide carbonyl, which is manifested after the rotation of the amide bond around

the C-2 – N1 and C-15 – C-16 bonds [33]. Moreover, we have observed by TLC that both RFQ and RFQ^{II} afford a reaction mixture with the same final composition (same FP composition) after bleaching with hydrogen peroxide. TLC (butanol/ethanol/water = 10:8:5) of FP contains at least four products with retardation factors of 0.59, 0.63, 0.70 and 0.84, which yield a strong fluorescent signal at λ= 366 nm (Figure S6). The likely unspecific nature of the reaction of ROS with RFQ (or RFQ^{II}), is consistent with the presence of several final products and made NMR characterization unviable. However, based on the loss of colour and antimicrobial properties of FP, we reason that the bleaching reaction could result in the loss of the naphthoquinone ring. Moreover, the mobility of the final products on the TLC using such a strong polar developing phase (butanol/ethanol/water = 10:8:5) also suggest the formation of polyhydroxylated substances and very likely N-oxides.

Table I – Chemical shift assignment for ^{1}H- and ^{13}C-NMR of CotA-laccase oxidation product which was identified as being rifampicin quinone (RFQ). See supplemental material for more details.

Position	δC	δH	H-H COSY	HMBC	H2BC
1	181.40			H-1'	
1'	128.55	7.78	H-3', H-5'	C-1, C-2, C-3, C-4	
2	137.16			H-1',	
2', 6'	50.09	2.61	H-3', H-5'	C-2', C-6', C-3', C-5'	H-3', H-5', C-3', C-5'
3	124.15			H-1'	
3', 5'	53.69	3.30	H-2', H-6'		H-2', H-6', C-2', C-6'
4	183.86			H-1'	
4'	45.76	2.37			
5	130.28			H-14	
6	166.61			H-14	
7	115.44			H-14	
8	172.63			H-14	
9	112.20			H-14	
10	110.16			H-14	
11	192.83			H-13	
12	107.25			H-13, H-28, H-29	
13	21.10	1.76		C-11, C-12	
14	7.67	2.28		C-5, C-6, C-7, C-8, C-9, C-10	
15	167.64			H-17, H-30	
16	128.99				
17	137.46	6.37	H-18, H-30	H-19, H-30, C- 15, C-18, C-19, C-30	H-18, H-30, C-18, C-30
18	124.81	6.80	H-17, H-19, H-20	H-17, H-19, H-30, C-16, C-17	H-17, H-19, C-17, C-19

19	143.02	5.93	H-18, H-20, H-30	H-17, H-20, H-21, H-30, H-31, C-17, C-18, C-20, C-21, C-31	H-18, H-20, C-18, C-20
20	38.56	2.45 – 2.40	H-18, H-19, H-21, H-31	H-19, H-21, H-31, C-18, C-19, C-21, C-31	H-19, H-21, H-31, C-19, C-21, C-31
21	71.35	3.86	H-20, H-22	H-19, H-20, H-22, H-22, H-23, H-31, H-32, C-19, C-20, C-23, C-32	H-20, C-20
22	33.12	1.77 – 1.70	H-21, H-23, H-32	H-23, H-32, H-24, C-21, C-23, C-25, C-32, C-33	H-32, C-23, C-32
23	77.64	3.00	H-22, H-24	H-22, H-25, H-32, H-33, C-21, C-22, C-25, C-32, C-33 or C-34	H-22, C-24
24	37.19	1.77 – 1.70	H-23, H-25, H-33	H-25, H-33, C-22, C-33 or C-34	H-23, H-33
25	74.26	5.13	H-24, H-26	H-23, H-26, H-33, H-34, H-36, C-23, C-24, C-26, C-27, C-33 or C-34, C-35	H-26, C-26
26	39.11	1.46 – 1.38	H-25, H-27, H-34	H-25, H-27, H-28, H-29, H-34, C-25, C-33 or C-34	H-25, H-34, C-25, C-34
27	77.12	3.43	H-26, H-28, H-29	H-25, H-28, H-29, H-34, H-37, C-25, C-26, C-28, C-29, C-34, C-37	H-28, C-28
28	118.19	5.06	H-27, H-29	H-27, H-29, C-12, C-26, C-27, C-29	H-27, H-29, C-27, C-29
29	141.42	6.08	H-27, H-28	H-13, H-27, H-28, C-12, C-26, C-27, C-28	H-28, C-28
30	20.78	2.09	H-17, H-19	H-17, C-15, C-16, C-17, C-18, C-19	H-17, C-17
31	17.22	0.86	H-20	H-19, H-20, C-19, C-20, C-21	H-20, C-20
32	11.70	1.03	H-22	H-21, H-22, H-23, C-21, C-22, C-23	H-22, C-22
33	8.88	0.54	H-24	H-22, H-23, H-25, H-26, H-27, C-23, C-24, C-25	H-24, C-24
34	8.83	0.13	H-26	H-22, H-23, H-25, H-26, H-27, C-25, C-26, C-27	H-26, C-26
35	172.42			H-25, H-36	
36	20.82	2.06		H-25, C-35	
37	57.48	3.08		H-27, C-27	
21-OH					
23-OH					
8-OH					
NH		10.48			

377

378 ***Assessment of the antimicrobial and toxicity properties of the final degradation products***

379 To assess the antimicrobial properties of the RIF, RFQ and FP, we have determined the

380 minimal inhibition concentrations (MICs) by the broth dilution method using an *E. coli* K12

MG1655 susceptible to RIF and four isogenic strains RIF resistant due to a single mutation in RpoB, a subunit of RNA polymerase - $RpoB^{H526Y}$, $RpoB^{S512F}$, $RpoB^{S531F}$ and $RpoB^{I572F}$ (Figure 4A). The susceptible strain has a MIC between 25 to ≥ 50 times more sensitive to RIF than the resistant RIF strains, confirming the antimicrobial properties of this antibiotic. RFQ still has antimicrobial properties since the MIC of the susceptible strain is between 12.5 to ≥ 25 times more sensitive to RFQ than the RIF-resistant strains. We noticed that RIF-resistant strains were also highly resistant to the RFQ suggesting a similar mode of action as RIF. Since the cytosol of *E. coli* is a very strong reducing environment, we hypothesize that a significant fraction of RFQ is likely to be reduced back to RIF inside the bacterial cells. Ascorbic acid and sodium dithionite are known to be strong reducers and, indeed, they reduce RFQ back to RIF, as observed by the purple colour of RFQ readily changing back to orange (typical of RIF) in the presence of either of these reducing agents. On the other hand, FP does not display antimicrobial properties since the MIC of the susceptible strain is very high and comparable to the RIF resistant strains (MIC > 500 µg/mL to all the strains). We have further corroborated that FP did not display antimicrobial properties by performing growth curves for the same strains in the presence of 100 µg/ml of RIF, RFQ and the final degradation FP (Figure 4B). While the susceptible strain is not able to grow in the presence of RIF and RFQ at these concentrations, it presents a comparable growth rate (*r*) to the RIF-resistant strains in the presence of FP ($r_{Susceptible}$ = 0.80 ± 0.09, r_{H526Y} = 0.96 ± 0.03, r_{S512F} = 0.65 ± 0.01, r_{S531F} = 0.84 ± 0.03, r_{I572F} = 0.80 ± 0.07; p = 0.293, one-way ANOVA).

To assess the effect of FP on the competitive fitness of each the RIF-resistant strains against the susceptible strain in the presence or absence of FP, we have mixed in a 1:1 ratio each of the resistance strain with the susceptible strain and grown for 24h at 37ºC in LB media or in LB supplemented with 100 µg/ml of FP (Figure 4C). The performance of the strains was assessed by plating both the initial mix and after 24h of growth simultaneously in LB plates (total

number of clones) and in LB supplemented with 100μg/mL rifampicin plates (resistance clones). The number of susceptible clones was calculated by subtracting the resistant clones from the total number. The susceptible strain outcompeted all the RIF-resistant strains both in presence and absence of FP ($p < 0.01$ to all of them, one-sample t-test), meaning that the numbers of resistant strains are expected to maintained low in the presence of FP. The relative fitness of the resistant strains in LB when competing against the susceptible strain was not influenced by the presence of FP when in competition with $RpoB^{H526Y}$ and $RpoB^{S512F}$ ($p = 0.15$ and 0.67, respectively; paired t-test). However, the fitness cost of the RIF resistant $RpoB^{S531F}$ and $RpoB^{I572F}$ mutants was slightly attenuated by the presence of FP in the LB ($p = 0.002$ and 0.003, respectively).

To assess the toxicity of the RIF and FP to eukaryotic cells, we conducted a bioassay with the model nematode organism *Caenorhabditis elegans* [26], previously demonstrated to be a trustworthy toxicity model [36]. We subjected *C. elegans* individuals to a concentration of 100 μg/mL of these compounds for 24 h and assessed their growth, by measuring the body area of the worms after that period (Figure 4D). The results show that the different treatments had no significant effect, apart from the negative control effect of lack of food (p-value < 0.001, multiple test correction), which indicates that neither RIF nor FP is toxic, at these concentrations, against *C. elegans* individuals. Thus, our results suggest that the proposed degradation pathway for rifampicin has potential for further industrial applications.

10.1002/cbic.202300627

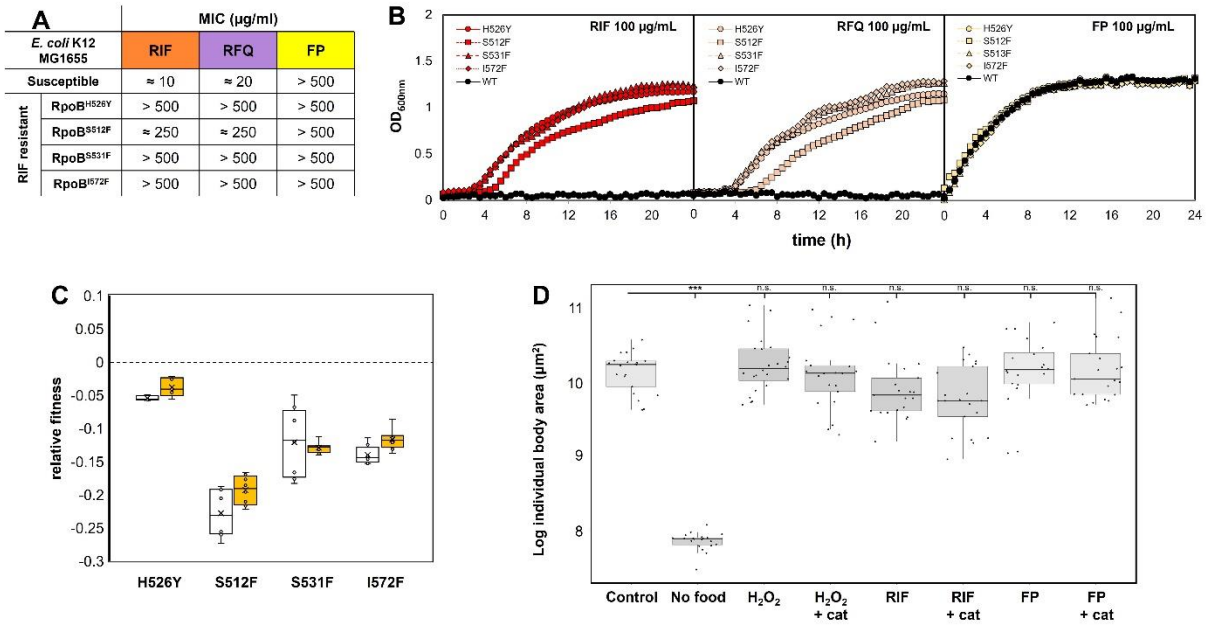

Figure 4 – Assessment of the antimicrobial and toxicity properties of the degradation products. A) Minimal inhibition concentrations (MICs) were determined for RIF, RFQ and the final degradation products by the broth dilution method using a *E. coli* K12 MG1655 susceptible to RIF and four isogenic strains RIF resistant due to a single mutation in RpoB, a subunit of RNA polymerase ($RpoB^{H526Y}$, $RpoB^{S512F}$, $RpoB^{S531F}$ and $RpoB^{I572F}$). **B)** Growth curves for the same strains as in A) in the presence of 100 µg/ml of RIF (left panel), RFQ (middle panel) and the final degradation products (right panel). **C)** Competition fitness assays in the presence or absence of FP between each of the RIF resistant strains against the susceptible strain in LB media (blank boxplot) or in LB supplemented with 100 µg/ml of FP (yellow boxplot). **D)** Toxicity of rifampicin and final product FP was assessed towards the growth of the model eukaryotic organism *C. elegans*.

CONCLUSIONS

Pharmaceuticals such as recalcitrant antibiotics are accumulating in rivers and wastewater. This problem contributes to the rise of antibiotic resistance, a worldwide problem to which no current solution exists. The two-step process we present in this work is an environmentally friendly procedure to transform the clinically relevant antibiotic rifampicin into non-antimicrobial compounds. Importantly, the final products of the degradation (FP) do not seem to favour the selection of RIF-resistant strains and are not toxic to the model organism *C. elegans*, which suggests that it would be safe to release FP into the environment. Despite the promising result, the applicability of this process for WWTPs could be improved by several

448 factors. Firstly, assessing of cost-effective application studies such as reusability and
449 immobilization of CotA-laccase in different matrices must be considered. Indeed, laccases have
450 been successfully immobilized in different matrices functionally and stably [13,37–40]. Secondly,
451 an assessment of the ability of this process to remove an increased scope of antibiotics would
452 be desirable. This scenario is probably possible, since several antibiotics present phenolic
453 and/or aromatic functional groups. Thirdly, further characterization of the main degradation
454 products is still required to ensure no toxicity to humans or animals. For instance, toxicity tests
455 of FP in mammals would be extremely desirable. Common antibiotic concentrations in the
456 water are usually low, on the order of the ng/L-µg/L, enough to select resistance against several
457 antibiotics [5,6]. On the other hand, this range of concentrations will result in extremely minimal
458 amounts of degradation products, significantly decreasing the risk of toxic effects on human
459 and animal health. Overall, our results suggest that we have developed a robust and
460 environmentally friendly process to effectively remediate rifampicin from antibiotic-
461 contaminated environments.
462

463 **ACKNOWLEGMENTS**

464 We acknowledge Dr. Isabel Gordo from Instituto Gulbenkian de Ciência (IGC) for kindly
465 providing the *E. coli* K12 MG1655 susceptible and rifampicin resistant strains.
466

467 **KEYWORDS**

468 Antibiotics
469 Bioremediation
470 Chemo-enzymatic transformation
471 CotA-laccase
472 Hydrogen peroxide

FUNDING

PD holds a Fundação para a Ciência e a Tecnologia (FCT) grant 2021.00778.CEECIND. IMC was supported by FCT through the grant UIDB/00329/2020. PK was funded by the European Union's Horizon Europe research and innovation programme under the Widening Participation and Spreading Excellence grant 101090282. IMC was supported by FCT through the grant UIDB/00329/2020. This work was supported by FCT - Fundação para a Ciência e a Tecnologia, I.P., through MOSTMICRO-ITQB R&D Unit (UIDB/04612/2020, UIDP/04612/2020) and LS4FUTURE Associated Laboratory (LA/P/0087/2020).

AUTHOR CONTRIBUTIONS

PD conceptualized the study. PD, PK and IMC performed the experiments and analysed the data. Project was supervised by PD while NMR experiments were supervised by MRV. Funding and resources were acquired by LOM. All authors reviewed and edited the final manuscript after an original draft written by PD.

COMPETING INTERESTS

The authors declare no conflict of interest.

REFERENCES

[1] J. C. Chee-Sanford, R. I. Mackie, S. Koike, I. G. Krapac, Y.-F. Lin, A. C. Yannarell, S. Maxwell, R. I. Aminov, *J. Environ. Qual.* **2009**, *38*, 1086–1108.

[2] J. L. Wilkinson, A. B. A. Boxall, D. W. Kolpin, K. M. Y. Leung, R. W. S. Lai, C. Galbán-Malagón, A. D. Adell, J. Mondon, M. Metian, R. A. Marchant, A. Bouzas-Monroy, A. Cuni-Sanchez, A. Coors, P. Carriquiriborde, M. Rojo, C. Gordon, M. Cara, M. Moermond, T. Luarte, V. Petrosyan, Y. Perikhanyan, C. S. Mahon, C. J. McGurk, T. Hofmann, T. Kormoker, V. Iniguez, J. Guzman-Otazo, J. L. Tavares, F. G. D. Figueiredo, M. T. P. Razzolini, V. Dougnon, G. Gbaguidi, O. Traoré, J. M. Blais, L. E. Kimpe, M. Wong, D. Wong, R. Ntchantcho, J. Pizarro, G.-G. Ying, C.-E. Chen, M. Páez, J. Martínez-Lara, J.-P. Otamonga, J. Poté, S. A. Ifo, P. Wilson, S. Echeverría-Sáenz, N. Udikovic-Kolic, M. Milakovic, D. Fatta-Kassinos, L. Ioannou-Ttofa, V. Belušová, J. Vymazal, M. Cárdenas-Bustamante, B. A. Kassa, J. Garric, A. Chaumot, P. Gibba, I. Kunchulia, S. Seidensticker, G. Lyberatos, H. P. Halldórsson, M. Melling, T. Shashidhar, M. Lamba, A. Nastiti, A. Supriatin, N. Pourang, A. Abedini, O. Abdullah, S. S. Gharbia, F. Pilla, B. Chefetz, T. Topaz, K. M. Yao, B. Aubakirova, R. Beisenova, L. Olaka, J. K. Mulu, P. Chatanga, V. Ntuli, N. T. Blama, S. Sherif, A. Z. Aris, L. J. Looi, M. Niang, S. T. Traore, R. Oldenkamp, O. Ogunbanwo, M. Ashfaq, M. Iqbal, Z. Abdeen, A. O'Dea, J. M. Morales-Saldaña, M. Custodio, H. de la Cruz, I. Navarrete, F. Carvalho, A. B. Gogra, B. M. Koroma, V. Cerkvenik-Flajs, M. Gombač, M. Thwala, K. Choi, H. Kang, J. L. C. Ladu, A. Rico, P. Amerasinghe, A. Sobek, G. Horlitz, A. K. Zenker, A. C. King, J.-J. Jiang, R. Kariuki, M. Tumbo, U. Tezel, T. T. Onay, J. B. Lejju, Y. Vystavna, Y. Vergeles, H. Heinzen, A. Pérez-Parada, D. B. Sims, M. Figy, D. Good, C. Teta, *Proc. Natl. Acad. Sci.* **2022**, *119*, DOI 10.1073/pnas.2113947119.

[3] A. Tello, B. Austin, T. C. Telfer, *Environ. Health Perspect.* **2012**, *120*, 1100–1106.

[4] P. Durão, R. Balbontín, I. Gordo, *Trends Microbiol.* **2018**, *26*, 677–691.

[5] E. Gullberg, S. Cao, O. G. Berg, C. Ilbäck, L. Sandegren, D. Hughes, D. I. Andersson, *PLoS Pathog.* **2011**, *7*, e1002158.

[6] C. Pereira, O. M. Warsi, D. I. Andersson, *Mol. Biol. Evol.* **2023**, *40*, msad010.

[7] C. J. Murray, K. S. Ikuta, F. Sharara, L. Swetschinski, G. R. Aguilar, A. Gray, C. Han, C. Bisignano, P. Rao, E. Wool, S. C. Johnson, A. J. Browne, M. G. Chipeta, F. Fell, S. Hackett, G. Haines-Woodhouse, B. H. K. Hamadani, E. A. P. Kumaran, B. McManigal, R. Agarwal, S. Akech, S. Albertson, J. Amuasi, J. Andrews, A. Aravkin, E. Ashley, F. Bailey, S. Baker, B. Basnyat, A. Bekker, R. Bender, A. Bethou, J. Bielicki, S. Boonkasidecha, J. Bukosia, C. Carvalheiro, C. Castañeda-Orjuela, V. Chansamouth, S. Chaurasia, S. Chiurchiù, F. Chowdhury, A. J. Cook, B. Cooper, T. R. Cressey, E. Criollo-Mora, M. Cunningham, S. Darboe, N. P. J. Day, M. D. Luca, K. Dokova, A. Dramowski, S. J. Dunachie, T. Eckmanns, D. Eibach, A. Emami, N. Feasey, N. Fisher-Pearson, K. Forrest, D. Garrett, P. Gastmeier, A. Z. Giref, R. C. Greer, V. Gupta, S. Haller, A. Haselbeck, S. I. Hay, M. Holm, S. Hopkins, K. C. Iregbu, J. Jacobs, D. Jarovsky, F. Javanmardi, M. Khorana, N. Kissoon, E. Kobeissi, T. Kostyanev, F. Krapp, R. Krumkamp, A. Kumar, H. H. Kyu, C. Lim, D. Limmathurotsakul, M. J. Loftus, M. Lunn, J. Ma, N. Mturi, T. Munera-Huertas, P. Musicha, M. M. Mussi-Pinhata, T. Nakamura, R. Nanavati, S. Nangia, P. Newton, C. Ngoun, A. Novotney, D. Nwakanma, C. W. Obiero, A. Olivas-Martinez, P. Olliaro, E. Ooko, E. Ortiz-Brizuela, A. Y. Peleg, C. Perrone, N. Plakkal, A. Ponce-de-Leon, M. Raad, T. Ramdin, A. Riddell, T. Roberts, J. V. Robotham, A. Roca, K. E. Rudd, N. Russell, J. Schnall, J. A. G. Scott, M. Shivamallappa, J. Sifuentes-Osornio, N. Steenkeste, A. J. Stewardson, T. Stoeva, N. Tasak, A. Thaiprakong, G. Thwaites, C. Turner, P. Turner, H. R. van Doorn, S. Velaphi,

A. Vongpradith, H. Vu, T. Walsh, S. Waner, T. Wangrangsimakul, T. Wozniak, P. Zheng, B. Sartorius, A. D. Lopez, A. Stergachis, C. Moore, C. Dolecek, M. Naghavi, *The Lancet* **2022**, *399*, 629–655.
[8] C. M. Morel, E. Mossialos, *BMJ* **2010**, *340*, c2115.
[9] M. B. Ahmed, J. L. Zhou, H. H. Ngo, W. Guo, N. S. Thomaidis, J. Xu, *J. Hazard. Mater.* **2017**, *323*, 274–298.
[10] A. C. Reis, B. A. Kolvenbach, O. C. Nunes, P. F. X. Corvini, *New Biotechnol.* **2020**, *54*, 34–51.
[11] A. C. Reis, B. A. Kolvenbach, O. C. Nunes, P. F. X. Corvini, *New Biotechnol.* **2020**, *54*, 13–27.
[12] D. Becker, S. Varela Della Giustina, S. Rodriguez-Mozaz, R. Schoevaart, D. Barceló, M. de Cazes, M.-P. Belleville, J. Sanchez-Marcano, J. de Gunzburg, O. Couillerot, J. Völker, J. Oehlmann, M. Wagner, *Bioresour. Technol.* **2016**, *219*, 500–509.
[13] Z. Wang, D. Ren, S. Jiang, H. Yu, Y. Cheng, S. Zhang, X. Zhang, W. Chen, *BMC Biotechnol.* **2021**, *21*, 47.
[14] G.-R. Wu, L.-J. Sun, J.-K. Xu, S.-Q. Gao, X.-S. Tan, Y.-W. Lin, *Molecules* **2022**, *27*, 8660.
[15] A. Koch, V. Mizrahi, D. F. Warner, *Emerg. Microbes Infect.* **2014**, *3*, 1–11.
[16] E. A. Campbell, N. Korzheva, A. Mustaev, K. Murakami, S. Nair, A. Goldfarb, S. A. Darst, *Cell* **2001**, *104*, 901–912.
[17] A. Telenti, P. Imboden, F. Marchesi, L. Matter, K. Schopfer, T. Bodmer, D. Lowrie, M. J. Colston, S. Cole, *The Lancet* **1993**, *341*, 647–651.
[18] L. O. Martins, P. Durão, V. Brissos, P. F. Lindley, *Cell. Mol. Life Sci.* **2015**, *72*, 911–922.
[19] A. C. Sousa, L. O. Martins, M. P. Robalo, *Molecules* **2021**, *26*, 3719.
[20] M. Bilal, S. S. Ashraf, D. Barceló, H. M. N. Iqbal, *Sci. Total Environ.* **2019**, *691*, 1190–1211.
[21] P. Durão, Z. Chen, A. T. Fernandes, P. Hildebrandt, D. H. Murgida, S. Todorovic, M. M. Pereira, E. P. Melo, L. O. Martins, *J. Biol. Inorg. Chem. JBIC Publ. Soc. Biol. Inorg. Chem.* **2008**, *13*, 183–193.
[22] L. O. Martins, C. M. Soares, M. M. Pereira, M. Teixeira, T. Costa, G. H. Jones, A. O. Henriques, *J. Biol. Chem.* **2002**, *277*, 18849–18859.
[23] F. J. Enguita, L. O. Martins, A. O. Henriques, M. A. Carrondo, *J. Biol. Chem.* **2003**, *278*, 19416–19425.
[24] A. J. Brenner, E. D. Harris, *Anal. Biochem.* **1995**, *226*, 80–84.
[25] R. W. Noble, Q. H. Gibson, *J. Biol. Chem.* **1970**, *245*, 2409–2413.
[26] L. J. Bischof, D. L. Huffman, R. V. Aroian, *Methods Mol. Biol. Clifton NJ* **2006**, *351*, 139–154.
[27] F. de J. N. dos Santos, V. F. Ximenes, L. M. da Fonseca, O. M. M. de Faria Oliveira, I. L. Brunetti, *Biol. Pharm. Bull.* **2005**, *28*, 1822–1826.
[28] M. Abdollahi, A. Hosseini, in *Encycl. Toxicol. Third Ed.* (Ed.: P. Wexler), Academic Press, Oxford, **2014**, pp. 971–974.
[29] C. J. Tredwin, S. Naik, N. J. Lewis, C. Scully, *Br. Dent. J.* **2006**, *200*, 371–376.
[30] T. Tzanov, S. A. Costa, G. M. Gübitz, A. Cavaco-Paulo, *J. Biotechnol.* **2002**, *93*, 87–94.
[31] J.-H. Chen, J.-W. Xu, C.-X. Shing, *J. Prosthet. Dent.* **1993**, *69*, 46–48.
[32] C. Torres, E. Crastechini, F. Feitosa, C. Pucci, A. Borges, *Oper. Dent.* **2014**, *39*, E261–E268.
[33] L. Cellai, S. Cerrini, A. Segre, M. Brufani, W. Fedeli, A. Vaciago, *J. Org. Chem.* **1982**, *47*, 2652–2661.

[34] Y. Jin, S. K. Gill, P. D. Kirchhoff, B. Wan, S. G. Franzblau, G. A. Garcia, H. D. H. Showalter, *Bioorg. Med. Chem. Lett.* **2011**, *21*, 6094–6099.
[35] L. Santos, M. A. Medeiros, S. Santos, M. C. Costa, R. Tavares, M. J. M. Curto, *J. Mol. Struct.* **2001**, *563–564*, 61–78.
[36] P. R. Hunt, *J. Appl. Toxicol.* **2017**, *37*, 50–59.
[37] null Hublik, null Schinner, *Enzyme Microb. Technol.* **2000**, *27*, 330–336.
[38] N. A. Kalkan, S. Aksoy, E. A. Aksoy, N. Hasirci, *J. Appl. Polym. Sci.* **2012**, *123*, 707–716.
[39] M. Mogharabi, N. Nassiri-Koopaei, M. Bozorgi-Koushalshahi, N. Nafissi-Varcheh, G. Bagherzadeh, M. A. Faramarzi, *Bioinorg. Chem. Appl.* **2012**, *2012*, 823830.
[40] M. Taheran, M. Naghdi, S. K. Brar, E. J. Knystautas, M. Verma, R. Y. Surampalli, *ACS Sustain. Chem. Eng.* **2017**, *5*, 10430–10438.

10.1002/cbic.202300627

606 **TABLE OF CONTENTS**

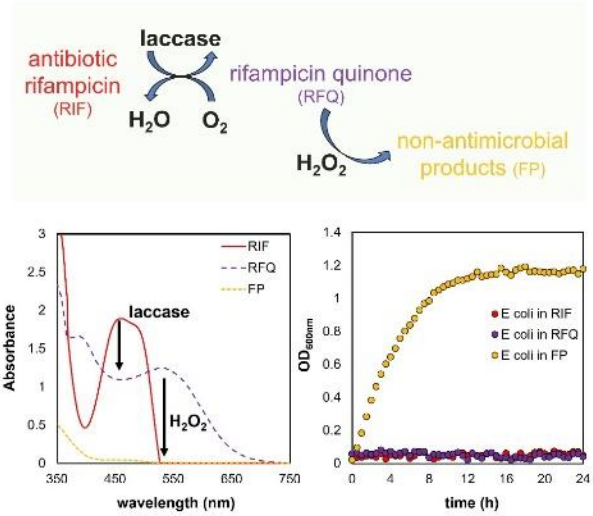

607

608 An environmentally friendly two-step process has been developed to effectively transform the
609 antibiotic rifampicin into non-antimicrobial compounds. The process involves an enzymatic
610 oxidation step by the bacterial CotA-laccase and a hydrogen peroxide bleaching step. NMR
611 identified rifampicin quinone as the main product of the enzymatic oxidation.

612